Proceeding *20th SEAGC - 3rd AGSSEA Conference in conjunction with 22nd Annual Indonesian National Conference on Geotechnical Engineering.* Jakarta - INDONESIA, 6 -7 November 2018. ISBN No. 978-602-17221-6-9

# Volcanic Cohesive Soil Behaviour under Static and Cyclic Loading

W. O. Sumartini[1], H. Hazarika[1], T. Kokusho[2] and S. Ishibashi[3]
[1]*Department of Civil Engineering, Kyushu University, Fukuoka, Japan*
[2]*Chuo University, Tokyo, Japan*
[3]*Department of Survey and Analysis, Nihon Chiken Co. Ltd., Fukuoka, Japan*
*E-mail*: waode_sumartini@yahoo.co.id

**ABSTRACT:** The objective of this study is to evaluate the behavior of reconstituted samples of a volcanic soil under static and cyclic loading using series of undrained static and cyclic test. The static test results show that at a low confining pressure, the soil exceeds contractive behavior followed by dilative behavior. This behavior indicates that the pore water pressure development is not higher than the soil shear strength. Otherwise, the soil shows contractive behavior. The cyclic test results show cyclic mobility behavior under an investigated cyclic stress ratio. In one hand, at low cyclic stress ratio, the shear strain increased slowly, and after a certain number of cyclic, it significantly increases. In another hand, the shear strain increases gradually at high cyclic stress ratio. These results indicate a contradictive behavior of the soil under different confining stress and cyclic stress ratio.
**Keywords:** Static triaxial test, cyclic triaxial test, volcanic soil, reconstituted samples, soil behavior.

## 1. INTRODUCTION

Historically, in Japan, some damages triggered by an earthquake on volcanic soil areas has been reported (Hazarika et al., 2018; Song et al., 2017; Kazama et al., 2012; Miyagi et al., 2011; Sassa, 2005). One of those area is Aso caldera in Kumamoto prefecture. The area suffered from widespread landslides which were triggered by the 2016 Kumamoto earthquake (Fig. 1). The landslides were concentrated in the Mount Aso area, within a 64 km radius of the epicenter. The 2016 Kumamoto earthquake is series of earthquakes which struck Kumamoto Prefecture of Kyushu Island on 14–16 April 2016. The foreshock earthquake occurred at 21.26 JST on 14 April 2016 at an epicentral depth of ~11 km at a magnitude (Mw) of 6.5 and the main shock struck at 01.25 JST on 16 April at an epicentral depth of ~10 km at an Mw of 7 (USGS). The source of the earthquakes was the activity of the Hinagu and Futagawa faults (GSI). These two faults experienced more than 2 m of strike-slip displacement at shallow depth. One of the landslides occurred near Aso Volcanological Laboratory of Kyoto University (Fig. 2). This landslide brought damage to houses (Fig. 3), public spaces and roads (Fig. 4). The inclination of the slope is about 10–15° Kochi et al. (2018) which is consistent with the value of 12° found by Song et al. (2017). In those landslides, several volcanic soil deposits have been found scattered on those slope. Sumartini et al. (2017) reported that the slope is composed of volcaniclastic deposits (Fig. 5) which visually have different colors and characteristics. The volcanic soil deposits came from different places as listed in Table 1. Song et al. (2017) and Kochi et al. (2018) stated that the landslide is composed of Kusasenrigahama pumice tephra beds (referred to as Orange soil in this paper). This Orange soil deposit, which acted as the slip surface of the landslide, is located on the top of Pre Takanoobane Lava pumice deposit (referred as Blackish soil). In one hand, from the map of resistivity distribution of the slope (Fig. 6) that has been drawn by Kochi et al. (2018), it can be concluded that the Orange soil which is located on the ground waterbed, is in saturated condition. In another hand, the resistivity map also shows that the Blackish soil is an impermeable deposit. Based on these fact, the authors presume that the Orange soil deposit was liquefied during the earthquake and becomes the main reason of the occurrence of the landslide.

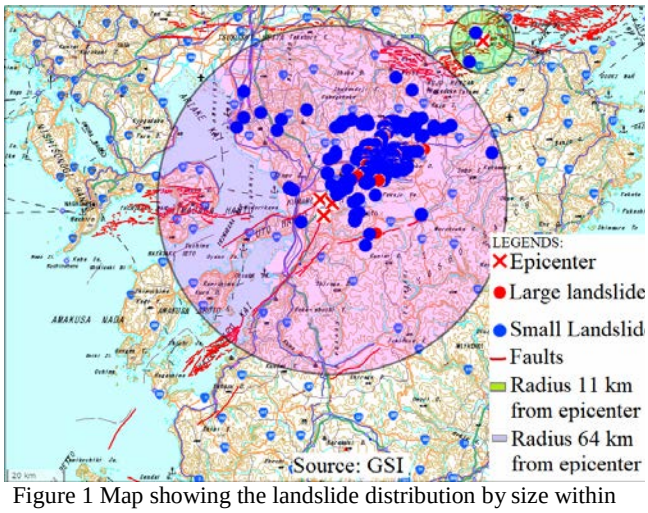

Figure 1 Map showing the landslide distribution by size within a 64 km radius of the Aso caldera (Sourced from GSI)

Figure 2 A massive landslide near Aso Volcanological Laboratory of Kyoto University


Figure 3 Swept away houses

Several studies related to the Orange soil were done and reported by Sumartini et al., (2017-2018). They studied chemical, mineral and microstructure characteristics as well as the behaviour of the Orange soil under static and cyclic loading. According to those studies, the landslide occured because the earthquake breakout the soil structure of the Orange soil deposit and led to liquefaction on that deposit. Several researchers have been studied the behavior of those volcanic soils due to earthquake by conducting triaxial cyclic tests (Ishikawa et al. in 2011, Suzuki and Yamamoto in 2004, Hatanaka et al. in 1985 and Sumartini et al. from 2017 to 2018). However, the behaviour of the Orange soil under cyclic loading in disturbed condition has not been done yet. Even though, the landslide occurred during the main shock, the deposit is not completely in undisturbed condition due to the foreshock. Thus, it is necessary to understand the behaviour of the Orange soil in disturbed condition. For that reason, series of undrained cyclic triaxial tests were performed to evaluate the behaviour of disturbed samples under cyclic loading. Finally, the results were compared with previous study and presented in this paper.

Figure 4 Damage to roads

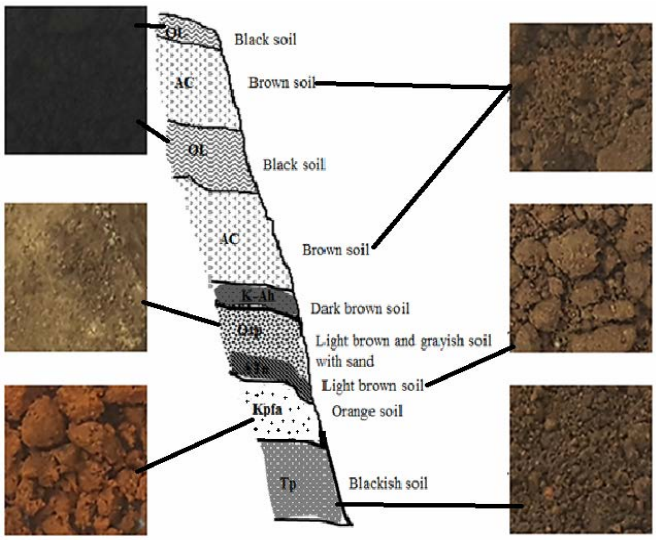


Figure 5 Schematic profile of the slope in Aso caldera (Modified from Sumartini et al. 2017)

Table 1 Origin of Volcanic Soil in Aso Saldera (Kochi et al., 2017).

| Deposit | Origin | Age (Cal ka) |
|---|---|---|
| Black soil | Organic (OL) | 10-present |
| Brown soil | Aso Central Cone Pumice (AC) | 7.3-10 |
| Dark brown soil | Kikai Akahoya Ash (K-Ah) | 7.3 |
| Light brown and grayish soil with sand | Otogase Lava Pumice (Otp) | 29-7.3 |
| Light brown soil | Aira Tn (Atn) | 29 |
| Orange soil | Kusasenrigahama Pumice (Kpfa) | 31 |
| Blackish soil | Takanoobane Lava Pumice (Tp) | 51±5 |

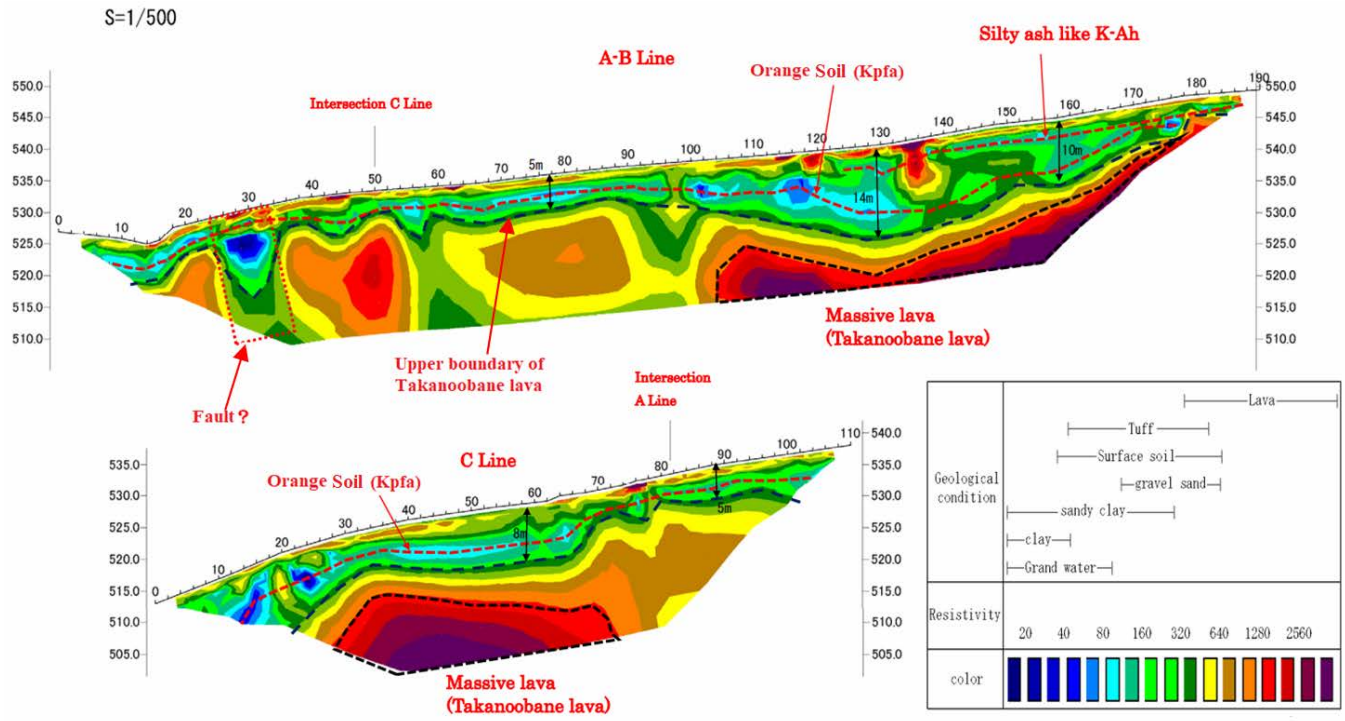


Figure 6 Resistivity distribution of the slope in Aso Volcanological Laboratory (Kochi et al., 2018)

## 2. MATERIAL PROPERTIES

The Orange soil is taken from the scarp of the slope near Aso Volcanological Laboratory. This soil contains about 60 percent of fine particles (Fig. 7) and based on its properties (Table 2) it can be classified as volcanic cohesive soil type II. It also contains 97 % by weight of feldspar mineral (Table 3) and has vesicular fabric. The fabric is composed of crystal flakes (Fig. 8). Sumartini et al. (2018[b]) idealized the flakes of the volcaniclastic deposit of the slope into flower type (Fig. 9a) and petal-type (Fig. 9b).

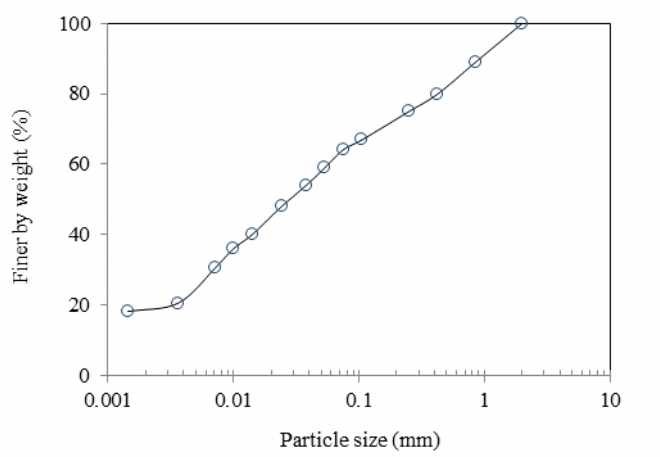


Figure 7 Grain Size distribution of the Orange soil (Sumartini et al., 2017)

Table 2 Physical Properties of Orange Soil (Sumartini et al., 2017)

| Physical Properties | Orange Soil |
|---|---|
| Specific Gravity | 2.24-2.38 |
| Dry Density, g/cm$^3$ | 0.51-0.58 |
| Wet Density, g/cm$^3$ | 1.23-1.30 |
| Water Content, % | 54.62-58.36 |
| Liquid Limit, % | 113.40 |
| Plastic Limit, % | 88.25 |
| Plasticity Index | 25.15 |

Table 3. Physical Properties of Orange Soil (Sumartini et al., 2018[a])

| Contents | Orange soil (Percent by weight) |
|---|---|
| Albite | 57 |
| Bytownite | 40 |
| Sodium hydrogen sulfide | 2.0 |
| Calcium copper germanium oxide | 1.4 |

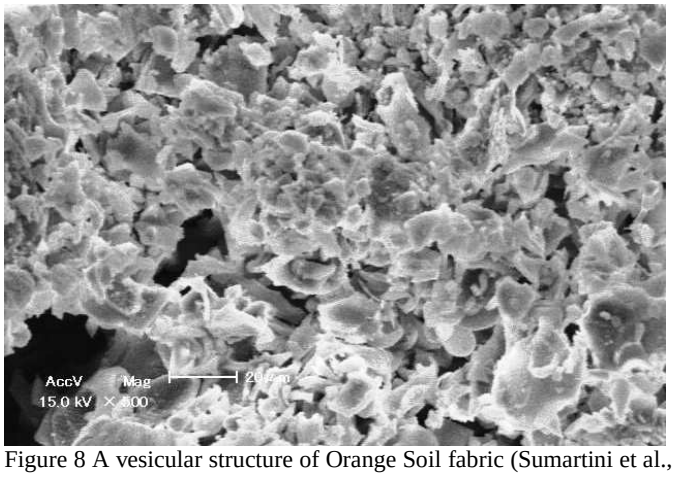


Figure 8 A vesicular structure of Orange Soil fabric (Sumartini et al., 2017)

(a) Petal-type (b) Flower type

Figure 9 Idealized crystal flake structures found in the deposits of the Aso Volcanological Laboratory Landslide. (a) Petal-type structure and (b) Flower type structure (Sumartini et al., 2018[b])

## 3. TESTING METHOD

Undrained cyclic triaxial tests were conducted on the Orange soil with 60 kPa of confining pressure. The disturbed samples were reconstituted from the undisturbed samples which have been tested. About 100 mm in height and 50 mm in diameter of the specimen have been produced using a steel mould. Double negative pressure and appropriate back pressure were applied to the samples and isotropically consolidated at the target effective pressure. B-values > 0.95 was ensured for all samples before shearing. The frequency of the cyclic axial load was 0.1 Hz for the undrained triaxial cyclic tests. To decide whether liquefaction occurred in this study or not, the pore water pressure ratio ($r_u$), define as the ratio of the pore water pressure to the normal stress, was used. When $r_u \geq 0.95$, the specimen was considered to have liquefied.

## 4. RESULTS AND DISCUSSION

### 4.1 Soil behavior under static loading

Figures 10 and 11 show respectively the stress-strain relation of disturbed and undisturbed samples in undrained static triaxial test. For disturbed samples, the deviatoric stress is rising gradually with the progress of axial strain for each confining pressure (Fig. 10). However, at low confining pressure, the peak is reached at large strain while at high confining pressure the peak is reached at small strain. For undisturbed samples, the deviatoric stress also is increasing gradually with the progress of axial strain, but when it reaches the peak with a specific strain, the deviatoric stress decreases (Fig. 11).

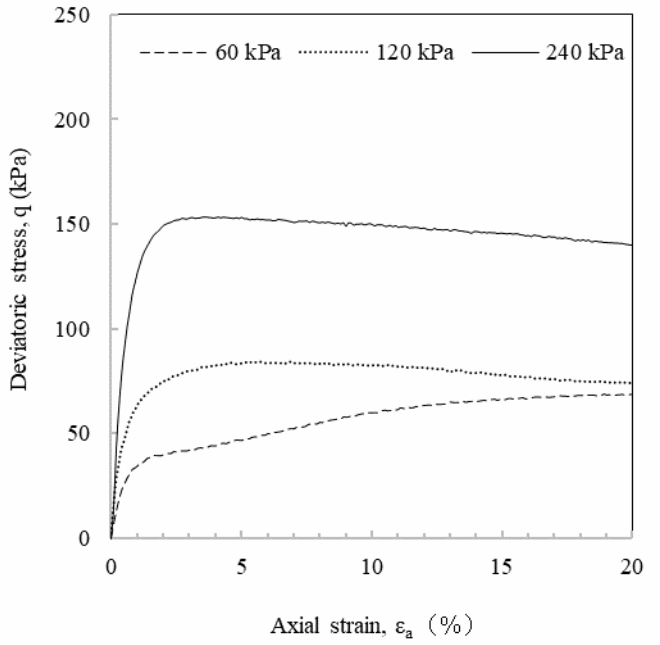


Figure 10 Stress versus axial strain of disturbed samples (Sumartini et al., 2018[a])

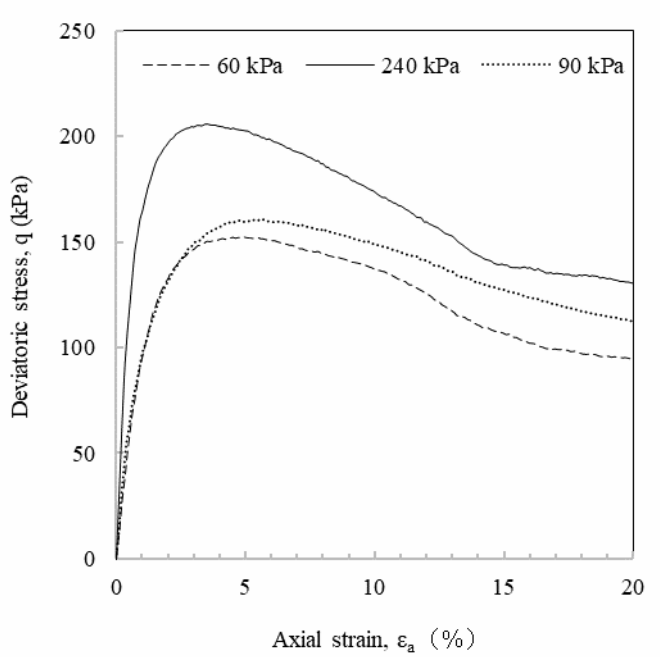


Figure 11 Stress versus axial strain of undisturbed samples (Sumartini et al., 2018[a])

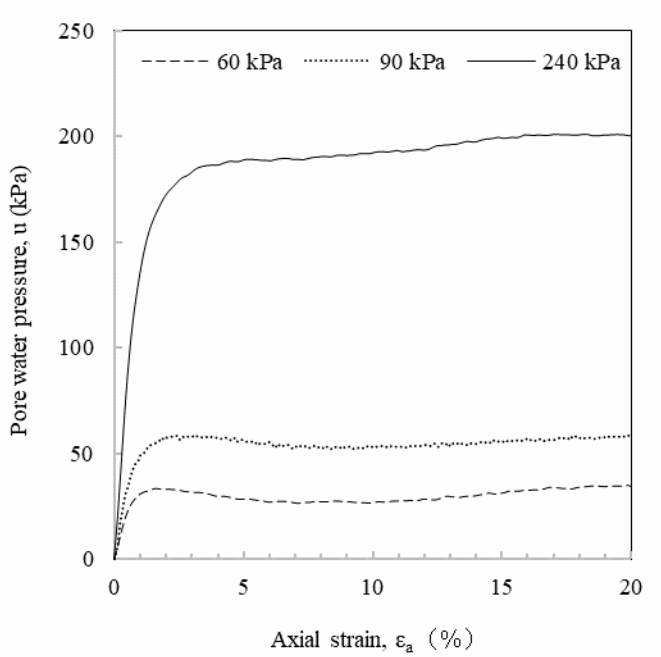


Figure 13 Pore water pressure versus axial strain of undisturbed samples (Sumartini et al., 2018[a])

Figures 12 and 13 display respectively the pore water pressure-strain relation of disturbed and undisturbed samples in the undrained static triaxial test. In low confining pressure, the pore water pressure is lower than the deviatoric stress and in high confining stress, the pore water pressure is higher compared to deviatoric stress. Consequently, when the confining pressure is low, the soil susceptibility to liquefaction is low. Otherwise, under high confining pressure, the soil has a high susceptibility to liquefaction.

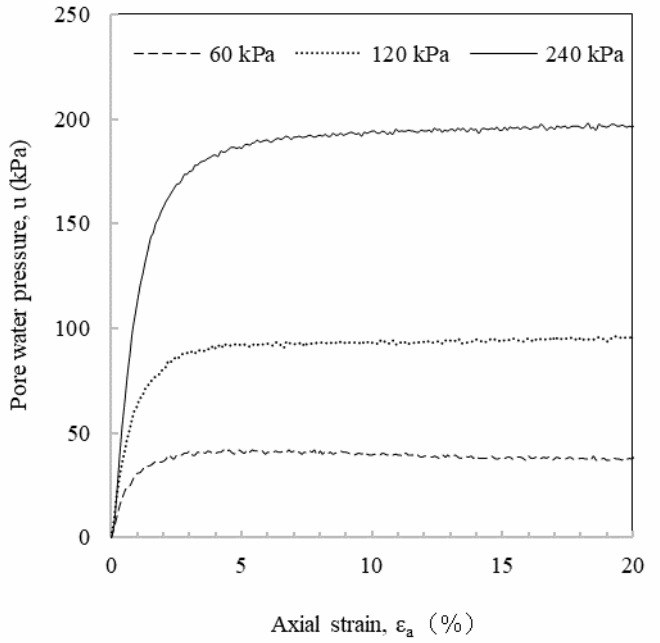


Figure 12 Pore water pressure versus axial strain of disturbed samples (Sumartini et al., 2018[a])

The behavior of the disturbed and undisturbed samples can be clearer by looking at the stress path of the soil as respectively shown in Figures 14 and 15. In one hand, under a low confining pressure, the disturbed sample is contracted and then dilated with no sign of temporary liquefaction. In contrary, under low confining pressure, the undisturbed sample is dilated, and when reaching the peak of the soil strength, the soil contracted. In another hand, under high confining pressure, disturbed and undisturbed samples show a contraction which means that they have a high susceptibility to liquefaction.

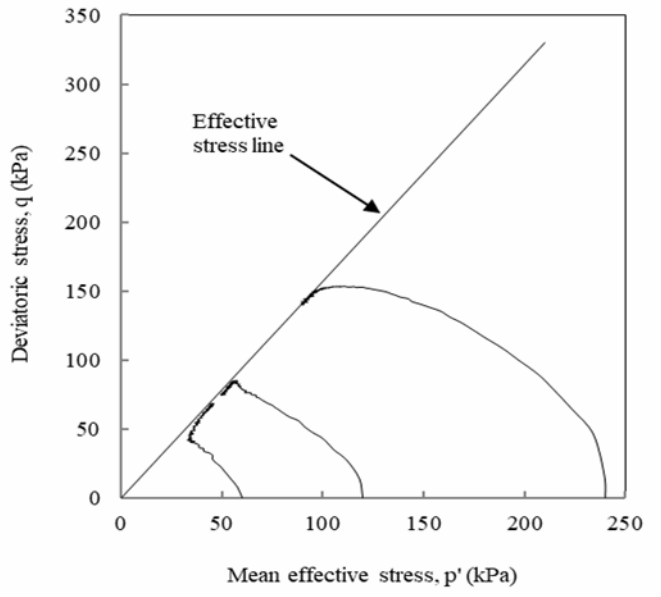


Figure 14 Stress path of the disturbed Orange soil samples (Sumartini et al., 2018[a])

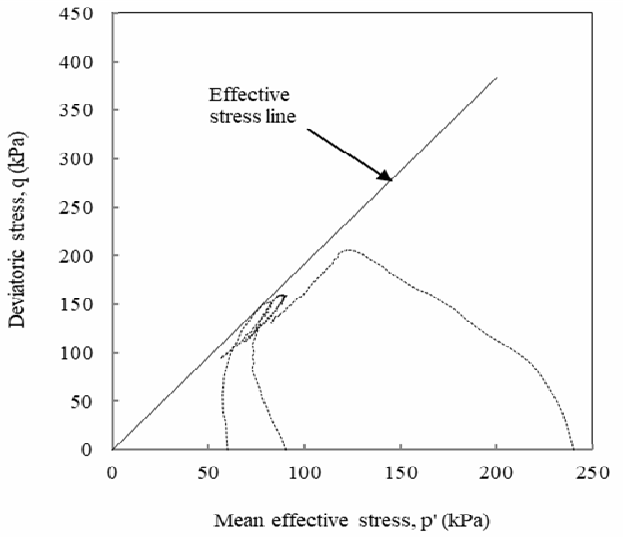


Figure 15 Stress path of the undisturbed Orange soil samples (Sumartini et al., 2018[a])

Figures 16 and 17 show the Mohr's stress circle of disturbed and undisturbed samples separately. The cohesion and the angle of the shear strength of total stress and effective stress are listed in Table 4. For disturbed samples, the cohesion of effective stress is about 1.48 times the total stress, and the angle is about 0.34 times the total stress. For undisturbed samples, the cohesion of effective stress is about 2.18 times the total stress while the angle is about 0.23 times the total stress. Finally, by comparing the cohesion and the angle of both type of samples, it can be concluded that the reconstitution process is reducing the cohesion by about 3.53 times for total stress and about 2.40 times for effective stress while the angle increases about 1.57 for total stress and about similar at effective stress.

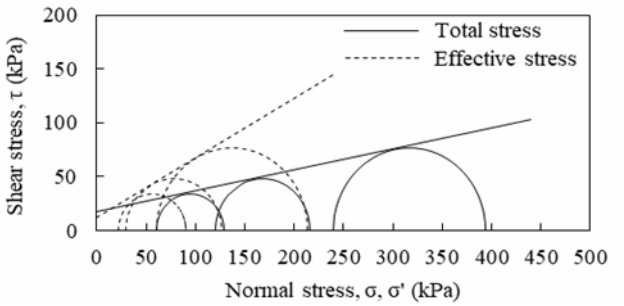


Figure 16 Mohr's Circle of disturbed samples

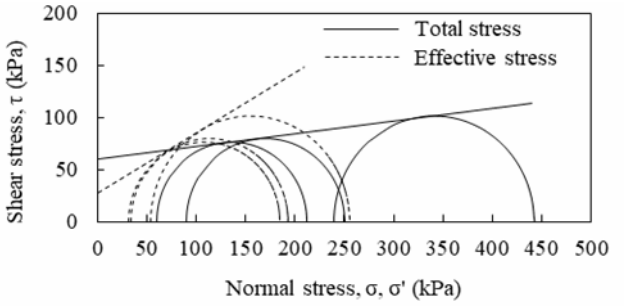


Figure 17 Mohr's Circle of undisturbed samples

Table 4 Strength Parameter of the Orange Soil

| Strength parameter | Disturbed | Undisturbed |
|---|---|---|
| $C_{cu}$ (kPa) | 17 | 60 |
| φ (°) | 11 | 7 |
| c' (kPa) | 11.5 | 27.5 |
| φ' (°) | 29 | 30 |

### 4.2 Soil behavior under cyclic loading

Figures 18 and 19 display the response of disturbed samples while Figures 20 and 21 show the response of undisturbed samples in the undrained cyclic triaxial test. The stress path trend of disturbed samples is similar to undisturbed sample although the disturbed sample appears faster in liquefying. The effective stress path of both samples indicates that the effective stress in undisturbed samples tends to decrease at a lower rate than in disturbed samples. The generation of excess pore water pressure for each cyclic load application is much faster for the disturbed samples compared to undisturbed samples. Therefore, it can be concluded that the deformation of the soil structure due to reconstituting process has a significant effect on the pore water pressure development. Thus, the disturbed samples appear to be more susceptible to liquefaction. The liquefaction susceptibility of disturbed samples and undisturbed samples are presented in Figure 22.

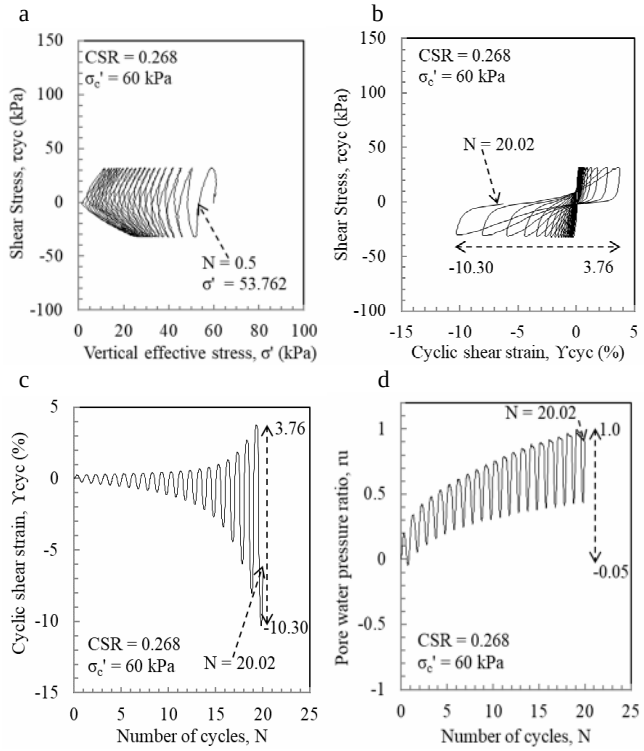


Figure 18 Soil response for CSR = 0.402: (a) effective stress path, (b) shear stress versus shear strain, (c) shear strain versus a number of cycles, and (d) pore water pressure ratio versus a number of cycles

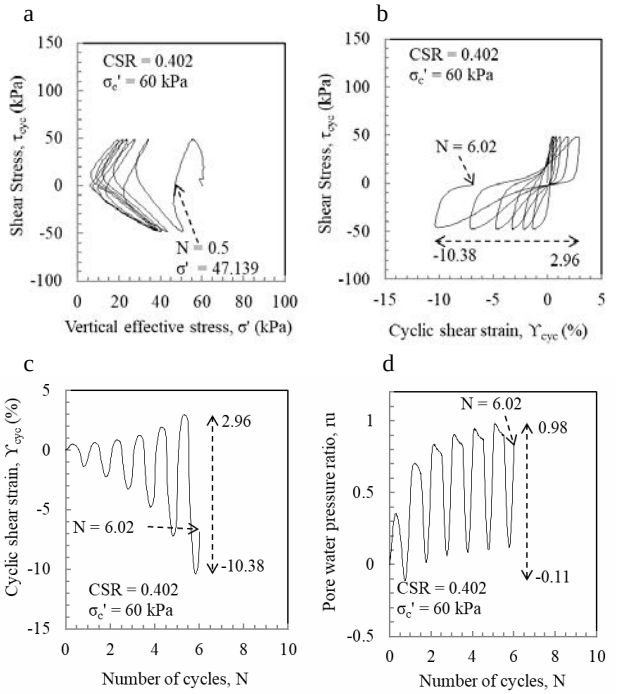


Figure 19 Soil response for CSR = 0.402: (a) effective stress path, (b) shear stress versus shear strain, (c) shear strain versus a number of cycles, and (d) pore water pressure ratio versus a number of cycles

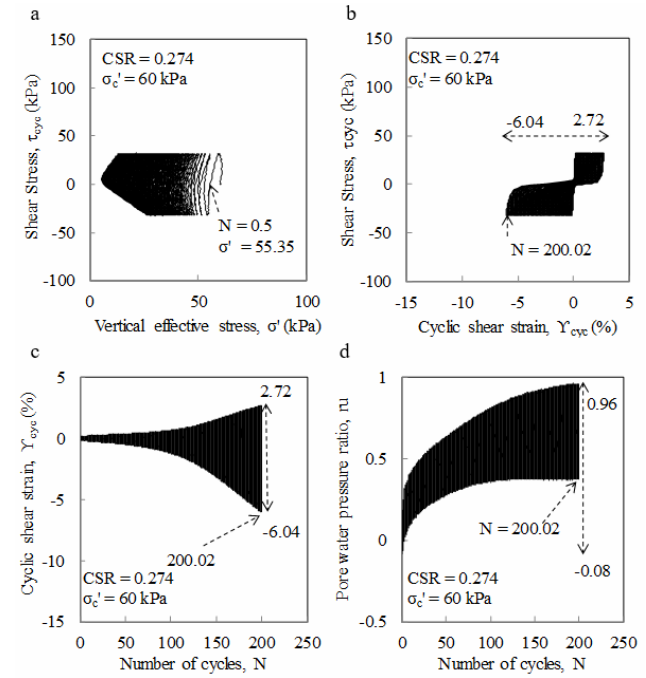


Figure 20 Soil response for CSR = 0.274: (a) effective stress path, (b) shear stress versus shear strain, (c) shear strain versus a number of cycles, and (d) pore water pressure ratio versus a number of cycles (Sumartini et al. 2018[a])

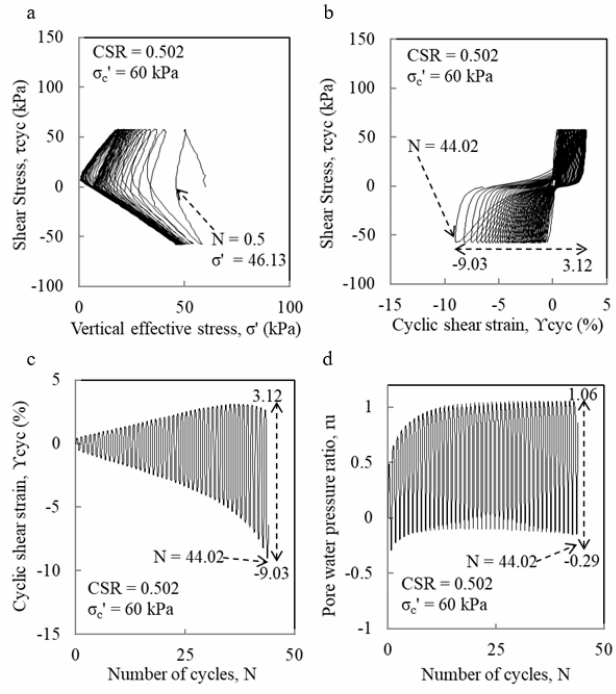


Figure 21 Soil response for CSR = 0.502: (a) effective stress path, (b) shear stress versus shear strain, (c) shear strain versus a number of cycles, and (d) pore water pressure ratio versus a number of cycles (Sumartini et al. 2018[a])

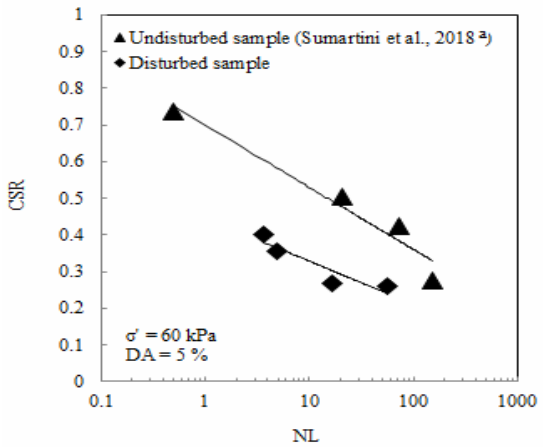


Figure 22 Liquefaction susceptibility of Orange soil: (a) undisturbed samples and (b) disturbed samples

### 4.3 Effect of cyclic loading to soil fabric

Figs. 23 and 24 respectively show the SEM analysis results of the Orange soil structure before and after the liquefaction tests (Sumartini et al., 2018). Fig. 13 shows that the soil structure is composed of a stack of the crystal flakes and is highly porous. In comparison, Fig. 14 shows that the soil structure is visibly broken, and a reduced crystal flake size. Consequently, the small flakes content of the fabric increases.

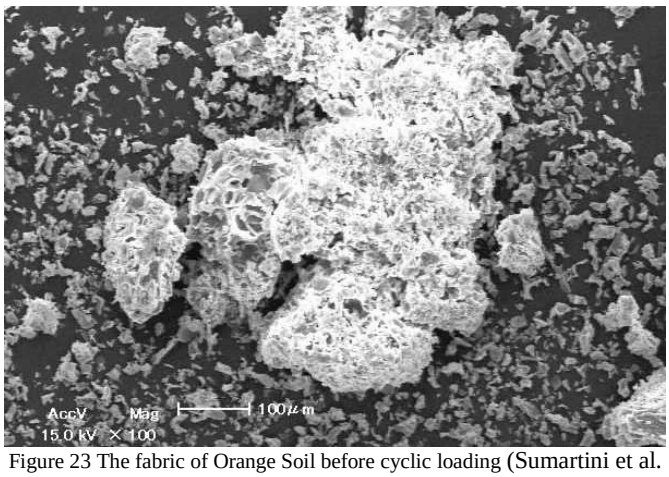


Figure 23 The fabric of Orange Soil before cyclic loading (Sumartini et al. 2018[a])

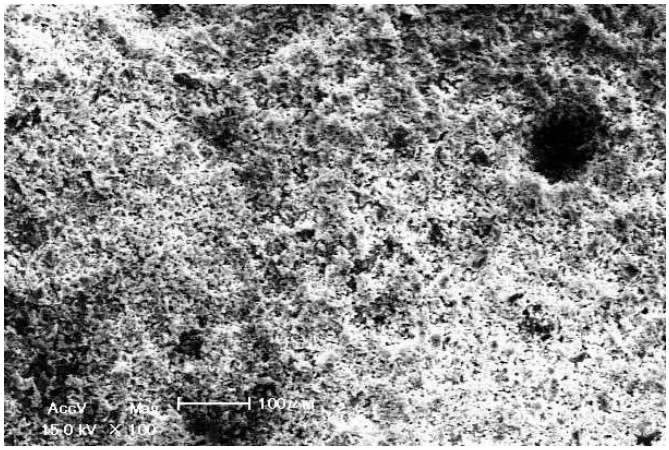


Figure 24 The fabric of Orange Soil before cyclic loading (Sumartini et al. 2018[a])

## 3. CONCLUSION

From the results of the investigation, the conclusions are made as following:

1. The Orange soil is a cohesive soil. The cohesion of the Orange soil is reduced after reconstituted.
2. The behavior of the disturbed samples under low confining pressure is contradictory with undisturbed samples. However, for high confining pressure, the behavior is similar. As the results, it can be concluded that the Orange soil deposit in small depth is less susceptible to liquefaction.
3. The slip surface is confirmed on the Orange soil layer deposit. Under cyclic loading, both samples show cyclic mobility behaviors under the CSR investigated. Although the CSR applied to disturbed samples quite lower than undisturbed samples, the disturbed samples appear significantly more susceptible to liquefaction compared to undisturbed samples. The results successfully describe the behavior of the Orange soil under cyclic loading. Also, the paper explains that the landslide occurred due to the liquefying of the Orange soil deposit triggered by the 2016 Kumamoto earthquake.
4. The cyclic loading affects the deformation of the soil fabric as confirmed by the reducing of the crystal flakes of the fabric in the SEM analysis.

## 4. ACKNOWLEDGMENT

The financial grant for this research under the J-RAPID program (Principal Investigator: Hemanta Hazarika) of Japan Science and Technology Agency (JST) is gratefully acknowledged. The first author is grateful to the Indonesia Endowment Fund for Education (LPDP) for financially supporting her study.

## 5. REFERENCES

Hatanaka, M., Sugimoto, M. and Suzuki, Y. (1985) "Liquefaction resistance of two alluvial volcanic soils sampled by in situ freezing". Soils and Foundations, 25, pp49-63.

Hazarika, H., Kokusho, T., Kayen, R.E., Dashti, S., Fukuoka, H., Ishizawa, T., Kochi, Y., Matsumoto, D., Hirose, T., Furuichi, H., Fujishiro, T., Okamoto, K., Tajiri, M. and Fukuda, M. (2017) "Geotechnical Damage due to the 2016 Kumamoto Earthquake and Future Challenges". Lowland Technology International, Special Issue on Kumamoto Earthquake and Disasters, 19, pp189-204.

Ishikawa, T., and Miura, S. (2011) "Influence of freeze-thaw action on deformation-strength characteristics and particle crushability of volcanic coarse-grained soils". Soils and Foundations, 51, pp785-799.

Kazama, M., Kataoka, S., and Uzuoka, R. (2012) "Volcanic Mountain Area Disaster Caused by the Iwate-Miyagi Nairiku Earthquake of 2008". Japan. Soil and Foundations, 52, pp168-184.

Kochi, Y., Kariya, T., Matsumoto, D., Hirose, T., and Hazarika, H. (2018) "Investigation of Slopes on The Takanoobane Lava Dome Using Resistivity Imaging Method". Lowland Technology International, Special Issue on Kumamoto Earthquake and Disasters, 19, pp 261-266.

Miyagi, T., Higaki, D., Yagi, H., Yoshida, S., Chiba, N., Umemura, J., and Satoh, G. (2011) "Reconnaissance Report on Landslide Disaster in Northeast following the M 9 Tohoku Earthquake". Landslides, 8, pp339-342.

Sassa. K. (2005) "Landslide disasters triggered by the 2004 Mid-Niigata Prefecture earthquake in Japan". Landslides, 4, pp113-122.

Song, K., Wang, F., Dai, Z., Iio, A., Osaka, O., Sakata, S. (2017) "Geological Characteristics of Landslides Triggered by the 2016 Kumamoto Earthquake in Mt. Aso Volcano, Japan". Bulletin of Engineering Geology and the Environment, Springer-Verlag, pp1-10.

[a]Sumartini, W. O., Hazarika, H., Kokusho, T., Ishibashi, S., Matsumoto, D., and Chaudhary, B. (2018) "Deformation and Failure Characteristics of Volcanic Soil at Landslide Sites due to the 2016 Kumamoto Earthquake". Lowland Technology International, Special Issue on Kumamoto Earthquake and Disasters, 19, March 2018, pp237-244.

[b]Sumartini, W. O., Hazarika, H., Kokusho, T., Ishibashi, S., Matsumoto, D., and Chaudhary, B., (2018) "Microstructural Characteristics of Volcanic Soil in Aso Caldera related to the Landslide Triggered by the 2016 Kumamoto Earthquake", Proceedings of 16th European Conference on Earthquake Engineering, Thessaloniki.

Sumartini, W. O., Hazarika, H., Kokusho, T., Ishibashi, S., Matsumoto, D. and Chaudhary, B., (2017) "Liquefaction Susceptibility of Volcanic Soil in Aso Caldera due to the 2016 Kumamoto Earthquake", Proceedings of the 19th International Summer Symposium, Fukuoka, pp13-14.

Suzuki, M., and Yamamoto, T., (2004) "Liquefaction characteristic of undisturbed volcanic soil in cyclic triaxial test". Proceedings of 13th World Conference on Earthquake Engineering, Vancouver, Paper No. 465.